

The potential energy landscape in the Lennard-Jones binary mixture model

This article has been downloaded from IOPscience. Please scroll down to see the full text article.

2003 J. Phys.: Condens. Matter 15 S1227

(<http://iopscience.iop.org/0953-8984/15/11/340>)

View [the table of contents for this issue](#), or go to the [journal homepage](#) for more

Download details:

IP Address: 171.66.16.119

The article was downloaded on 19/05/2010 at 08:25

Please note that [terms and conditions apply](#).

The potential energy landscape in the Lennard-Jones binary mixture model

M Sampoli¹, P Benassi², R Eramo², L Angelani³ and G Ruocco³

¹ Dipartimento di Energetica and INFN, Università di Firenze, Via Santa Marta 3, I-5019, Firenze, Italy

² Dipartimento di Fisica and INFN, Università di L'Aquila, Via Vetoio, Coppito, Aquila, Italy

³ Dipartimento di Fisica and INFN, Università di Roma 'La Sapienza', Piazzale Aldo Moro 2, I-00185, Roma, Italy

Received 4 December 2002

Published 10 March 2003

Online at stacks.iop.org/JPhysCM/15/S1227

Abstract

The potential energy landscape in the Kob–Andersen Lennard-Jones binary mixture model has been studied carefully from the liquid down to the supercooled regime, from $T = 2$ down to 0.46. One thousand independent configurations along the time evolution locus have been examined at each temperature investigated. From the starting configuration, we searched for the nearest saddle (or quasi-saddle) and minimum of the potential energy. The vibrational densities of states for the starting and the two derived configurations have been evaluated. Besides the number of negative eigenvalues of the saddles other quantities show some signature of the approach of the dynamical arrest temperature.

1. Introduction

In recent years a considerable research effort has been devoted to attempts to understand the complex phenomenology of supercooled glass-forming liquids and in particular the enormous increase in relaxation times and viscosity, by many orders of magnitude, that occurs upon decreasing the temperature. It was Goldstein [1] who first related the behaviour of glass formers to the underlying potential energy landscape (PEL) and proposed characterizing the dynamics of the system through the motion of a point in the complex high-dimensional PEL ($3N$ -dimensional if N is the total number of particles). Further, he suggested focusing on the PEL local minima where the system is supposed to be trapped at low enough temperatures. At low temperatures, but above the glass transition, the phase space spanned by the system at equilibrium can ideally be characterized by two different types of process: a 'fast' relaxation into local minima (or basins) and the 'slow' relaxation due to the crossing between loosely connected basins (the so-called 'hopping' from basin to basin even if, in the classical mechanics PEL language, there exist only tortuous and crooked routes connecting two admissible basins). Goldstein focused attention on the minima of the PEL, but before the system spends much time

in a given basin, there are situations where ‘fast’ and ‘slow’ relaxations are not recognizable, the diffusion is still substantial, and a lot of minima are visited in a continuous way. In this case, one attempts to relate the diffusion dynamics to unstable directions in equilibrium (or instantaneous) PEL configurations, i.e. in the context of the instantaneous normal-mode approach [2, 3]; however, special points other than PEL minima are found to characterize the dynamics of the system better: they are the minima of the squared modulus of the gradient of the potential energy, i.e. saddles (absolute minima) and what we call ‘quasi-saddles’ (local minima). Indeed the unstable directions of a saddle give some information about the number of different minima existing in that PEL region and therefore about the diffusion processes. In the past, the relevance of saddles to the dynamics of glassy systems had already been recognized in the context of mean-field spin glasses [4, 5]. A large number of recent works have renewed interest in the PEL and its characterization through saddle points and minima, in order to achieve a better understanding of the continuous transition from liquid to glass [6–10].

The purpose of the present work is to investigate in detail the statistical properties of the PEL of a binary Lennard-Jones system from the liquid down to the supercooled regime near the structural arrest. To do that, a set of temperatures above the glass transition have been considered and for each of them a set of independent configurations have been examined. Nearest saddles and minima have been searched for and the normal-mode analysis has been performed for all configurations.

2. Numerical computations

The system under consideration is a binary mixture of classical particles. The system is the same as that considered by Kob and Andersen [11], apart from a detail in the truncation of the potential. The mixture is made up of 256 particles, 205 of type *A* and 51 of type *B* (about 80% of type *A* and 20% of type *B*). Particles *A* and *B* have the same mass and interact with each other via a Lennard-Jones potential, i.e. $V_{\alpha\beta}(r) = 4\epsilon_{\alpha\beta}[(\sigma_{\alpha\beta}/r)^{12} - (\sigma_{\alpha\beta}/r)^6]$ with $\alpha, \beta \in \{A, B\}$. The parameters of the potentials are $\epsilon_{AA} = 1.0$, $\sigma_{AA} = 1.0$, $\epsilon_{BB} = 0.5$, $\sigma_{BB} = 0.88$, $\epsilon_{AB} = 1.5$, $\sigma_{AB} = 0.8$. In the following, all the results will be given in reduced units, i.e. length in units of σ_{AA} , energy in units of ϵ_{AA} , temperature in units of k_B/ϵ_{AA} , and time in units of $(m_A\sigma_{AA}^2/\epsilon_{AA})^{1/2}$.

The interaction potential at long distances is tapered in the range $0.95r_2 = r_1 \leq r \leq r_2 = 2.56\sigma_{AA}$ with the following fifth-order smoothing function: $\mathcal{T}(r) = 1 + (r_1 - r)^3(6r^2 + (3r + r_1)(r_1 - 5r_2) + 10r_2^2)/(r_2 - r_1)^5$. In this way the potential, the forces, and their derivatives are continuous and it is possible to keep the energy constant to better than $1/10^5$ over 100 millions of molecular dynamics (MD) time steps near the critical temperature. The MD simulation was performed in the *NVE* ensemble using the leapfrog algorithm with a time step of 1.5×10^{-3} at temperature above $T = 1.0$ and of 2×10^{-3} at lower temperatures. A neighbour list was used to speed up the calculation.

In their paper, Kob and Andersen [11] truncated and shifted the potential at a cut-off distance of $2.5\sigma_{\alpha\beta}$. In the uniform density approximation, our tapering corresponds to an average cut-off distance of about $2.5\sigma_{AA}$, and the resulting potential energy is shifted (downward) by only about 0.56 energy units with respect to the values quoted⁴.

First the configurations were produced at high temperature and then thermalized at the highest temperature investigated ($T = 2.0$). The initial configurations at lower temperatures were obtained in sequence by cooling and thermalizing previous configurations at different

⁴ The shift value is dependent slightly on temperature and configuration (‘*I*’, ‘*W*’ or ‘*V*’; see the text); the variation is less than ± 0.01 energy units.

temperatures (1.8, 1.6, 1.4, 1.2, 1.0, 0.9, 0.8, 0.7, 0.6, 0.5, 0.48, 0.46). Not all the configurations were analysed in full detail.

For each temperature, 1000 independent configurations were stored and then analysed. The minimum number of steps required between two subsequent configurations for them to be independent was determined in test runs. Two subsequent configurations are classified as independent if different potential minima are always obtained practically. We used a separation of 1000 steps at high temperatures down to $T = 1.0$, then we increased this number following the viscosity trend, so we used 10^4 steps at $T = 0.7$ and 10^5 steps at $T = 0.46$. The procedure is similar to that used to study the inherent dynamics by Schroeder *et al* [12].

To characterize the states of the supercooled binary mixture, we searched for the nearest saddle point (' W ') and the nearest minimum (' V ') of the PEL from the initial equilibrium (' I ') configurations. The saddle (or quasi-saddle as explained subsequently) configurations correspond to minimizing the sum of the squared forces, i.e. $W = |\nabla V|^2$ where V is the sum of all interaction potentials of our system and ∇ is the gradient for all the particle coordinates. If $|\nabla V|^2$ is really vanishing, i.e. is an absolute minimum, the configuration corresponds to a real saddle; otherwise we call it a quasi-saddle since usually there is only one direction with a zero or nearly zero eigenvalue and a non-zero force [13]. The minima of V are always absolute minima of $|\nabla V|^2$.

To obtain good nearest configurations of W - and V -minima from an initial equilibrium configuration of our system of 256 particles is a very difficult problem. The details of the two search procedures that we used are lengthy and will be described elsewhere [14]⁵. Here we want to stress that various standard algorithms have been employed during the search and various criteria have been adopted for switching among the different algorithms. From the numerical point of view, the minima obtained are quite satisfactory. Indeed at the start, the value of $|\nabla V|^2$ is of the order of 10^7 (in internal MD units) while at the minimum of W it is in the range 10^{-1} – 10^2 for quasi-saddles and in the range 10^{-8} – 10^{-2} for true saddles. At the minimum of V it is always less than 10^{-3} (in the range 10^{-8} – 10^{-2}). In the worst case, the value of $|\nabla V|^2$ is reduced by a factor of 10^5 . This happens when the point of inflection is on a steeply sloping surface.

In figure 1 we plot the distribution of $|\nabla V|^2$ at the W -minima for two extreme values of temperature. It should be noted that:

- (i) the temperature strongly affects the distribution;
- (ii) the number of true saddles (for which $|\nabla V|^2$ is vanishing) is strongly decreasing with temperature;
- (iii) the force residuals, i.e. $|\nabla V|^2$ values, are larger at low temperatures in contrast to what one can expect intuitively.

Moreover the temperature variation of the distribution is nearly confined to the low-temperature side (below $T = 1.0$). The second point is the reason that it becomes more and more difficult to analyse the low-temperature data by using only those configurations which have the W -minima as true saddles. Therefore we choose to analyse all the configurations and to inspect whether true saddles and quasi-saddles share the same pieces of information.

⁵ A brief sketch is as follows. All the programs tested for finding minima in a multidimensional space (768 dimensions in our case) stick at some points when a tortuous deep valley is encountered. Usually they decrease the step more and more, and the search becomes very slow and possibly stops. The procedure can be tested easily in the case of ' V '-minima, because a potential minimum requires the sum of the squared forces to be zero and the Hessian matrix to have all positive eigenvalues (except three zeros). Different algorithms usually stick at different points and the same algorithm with a larger step can be effective in overcoming some critical situations. Therefore a complex flow chart with different algorithms (steepest descent, Gauss–Newton, Levenberg–Marquardt, preconditioned conjugate gradient, etc) was used. In both ' W '- and ' V '-minima we started with a steepest descent search.

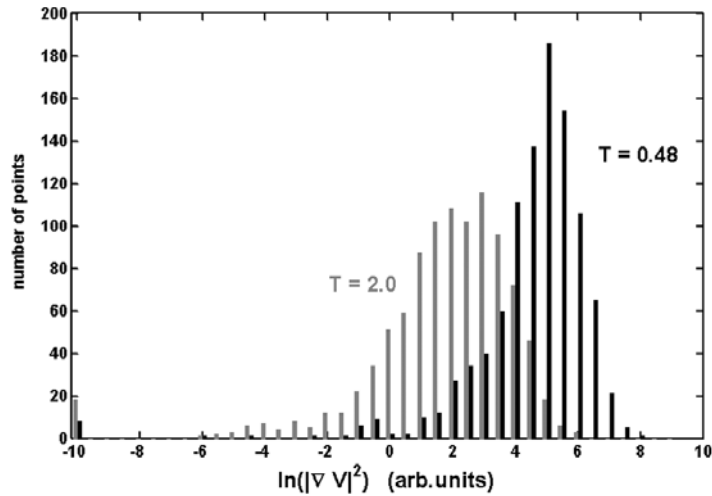


Figure 1. The distribution at high ($T = 2.0$, black lines) and low ($T = 0.48$, grey lines) temperatures of the $|\nabla V|^2$ values for W -minimization. True saddles are grouped around the value -10 of $\ln(|\nabla V|^2)$.

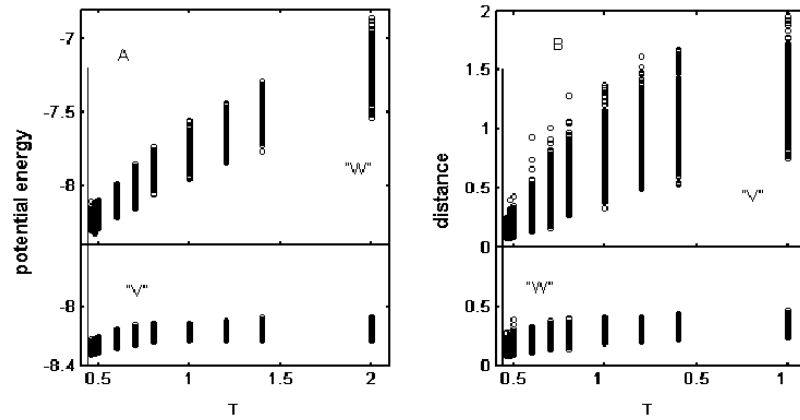


Figure 2. Panel A, on the left: potential energy (internal units) of quasi-saddles (' W ', upper part) and potential minima (' V ', lower part) versus temperature. Panel B, on the right: Cartesian distance in box units of potential minima (' V ', upper part) and quasi-saddles (' W ', lower part) from the starting equilibrium configuration versus temperature. The thin vertical line, in both panels, is drawn at $T_c = 0.435$.

3. Analysis of the results

3.1. Behaviour of potential energy at minima and saddles

In figure 2 we have reported the behaviour of the potential energy versus temperature for the quasi-saddles (' W ') and minima (' V '). As one can see, the potential energy of ' W ' is decreasing rapidly with temperature while that of ' V ' is practically constant, as already reported in [6]. On getting closer to the temperature of structural arrest, even the ' V '-potential energy becomes a decreasing function of the temperature, as has already been shown by Sastry *et al* [15].

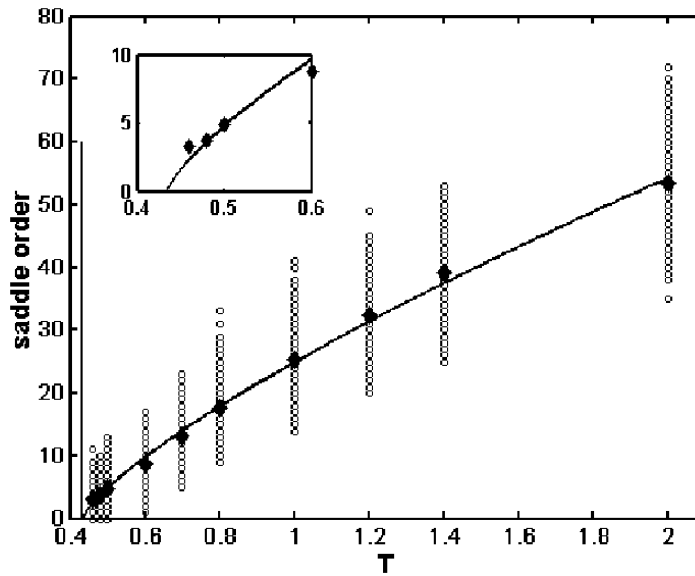


Figure 3. The saddle order (number of negative eigenvalues) for each quasi-saddle configuration at different temperatures. Full diamonds represent average values. The solid curve is a power law fit to average values: $\text{constant} \times (T - T_c)^\gamma$ with $\text{constant} \simeq 38.5$, $T_c \simeq 0.435$, $\gamma \simeq 0.77$. A solid vertical line is drawn at T_c . In the inset a blow-up of the lowest-temperature data is shown.

In the right-hand panel of the same figure we have shown the Cartesian distances (in box units) of ‘V’ and ‘W’ from the starting equilibrium configurations. In that case the temperature behaviour of the two kinds of minimum is reversed between ‘V’ and ‘W’, i.e. the average distances of quasi-saddles from equilibrium configurations are practically temperature independent while those of minima strongly decrease with decreasing temperature. This kind of behaviour can be expected because the potential energy of the starting equilibrium configurations is known to be nearly proportional to temperature [6] and configurations that are not very ‘distant’ from equilibrium are reasonably dependent on temperature.

In figure 3 we plot the number of negative eigenvalues of the Hessian matrix at quasi-saddle points versus temperature. This number goes quickly to zero at the critical temperature, i.e. the temperature of structural arrest, as already found by a similar analysis performed in [6, 7]. A solid vertical line in the figure represents the value of the mode coupling critical temperature [16] ($T_c \simeq 0.435$) derived from the power law behaviour of the diffusion constant [11]. The same value is obtained by a power law fitting of saddle order versus temperature (the solid curve in figure 3). This confirms the number of negative eigenvalues of quasi-saddles (or saddles) to be strictly connected with the diffusion constant. In contrast, a negative eigenvalue of an equilibrium configuration, i.e. a negative curvature of the instantaneous potential energy, is not always connected with a path joining two different minima, i.e. a diffusion path.

3.2. Quasi-saddles characteristics

As already noted in [7], the quasi-saddles at different temperatures explore different regions of the PEL. Therefore at low temperatures we have low values of the potential energy of ‘W’ together with low numbers of negative eigenvalues, as shown in figure 4.

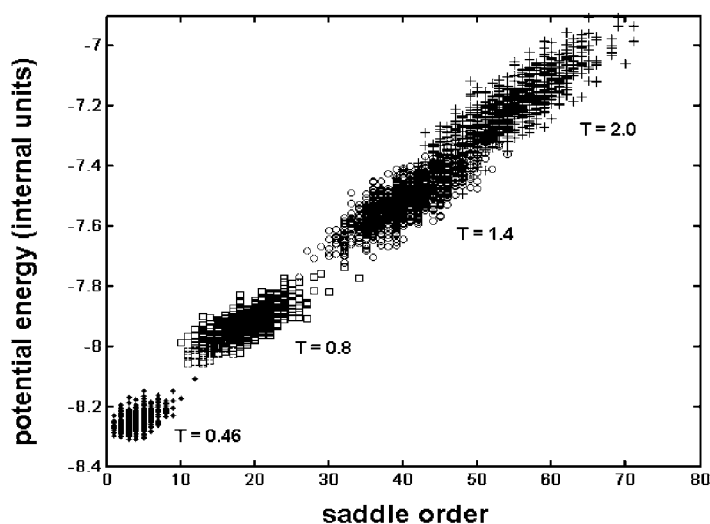


Figure 4. Potential energy of quasi-saddles versus saddle order (number of negative eigenvalues) at some chosen temperatures: $T = 0.46$ (full diamonds), $T = 0.8$ (open squares), $T = 1.4$ (open circles), and $T = 2.0$ (plus signs).

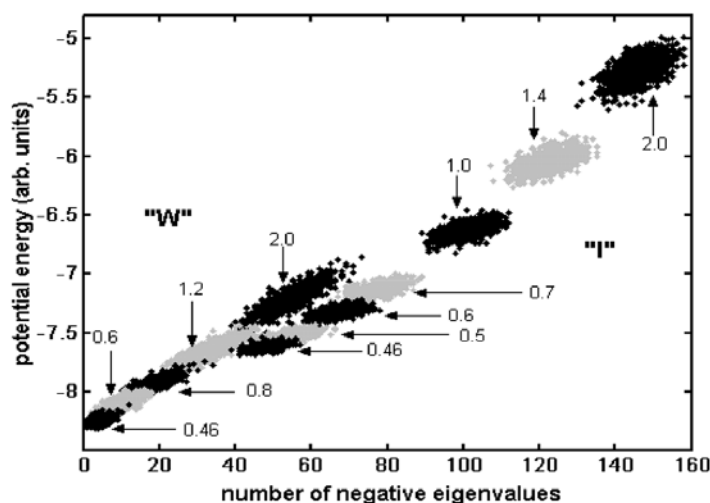


Figure 5. Potential energy for initial equilibrium configurations (' I ') and quasi-saddles (' W ') versus number of negative eigenvalues at the temperatures indicated.

We underline that the potential energy itself is not sufficient to determine the number of negative eigenvalues of the Hessian matrix. Indeed even at the same value of the potential energy, the number of negative eigenvalues is substantially different for quasi-saddles (' W ') and initial equilibrium configurations (' I '), as shown in figure 5 where we plotted the potential energy of ' I ' and ' W ' versus the number of negative eigenvalues at different temperatures. From the values and distribution in energy of ' I ' and ' W ' at the same temperature, we can easily derive that the enormous decrease of diffusion (and increase in viscosity) lowering the

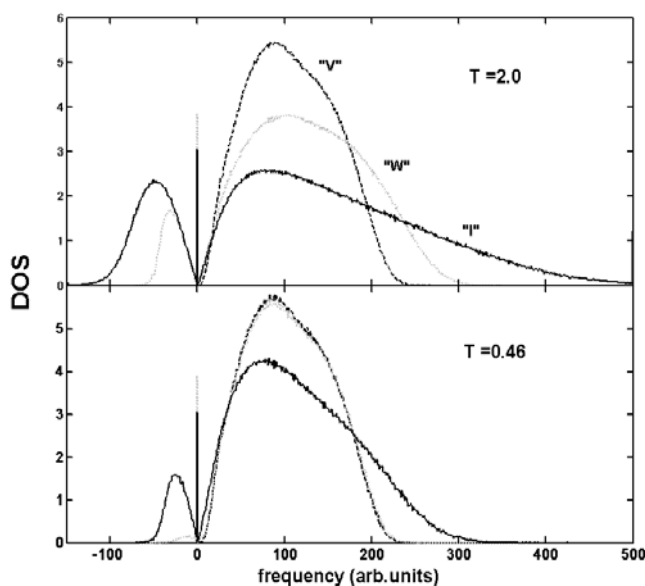


Figure 6. The upper panel: the average DOS at high temperature in the liquid regime from the normal-mode analysis performed on the three different configurations, ‘I’ (solid curve), ‘W’ (dotted grey curve), and ‘V’ (dashed curve). The lower panel: the same average DOS is shown near T_c in the supercooled regime. Imaginary frequencies (square roots of negative eigenvalues) are reported as negative frequencies. In the channel around zero of the histogram, we found the three zero-frequency eigenvalues (connected to translational invariants); for quasi-saddles, another zero-frequency eigenvalue is found due to the change of curvature in one direction of the potential energy hypersurface ($3N = 768$ dimensions). In the supercooled regime, approaching T_c , the ‘W’-DOS becomes more and more similar to the ‘V’-DOS.

temperature in the supercooled regime is due essentially to entropic barriers, i.e. to difficulties in reaching the saddle points, and not to activated processes [17]⁶.

3.3. Spectral densities of potential minima, saddles, and initial configurations

To better understand the modifications of the PEL around ‘I’-, ‘W’-, and ‘V’-configurations that occur on lowering the temperature, we have studied the frequency distribution of the vibrational states derived from the Hessian matrix of the potential energy. To show all the spectral features in a single plot, the eigenfrequencies of unstable directions (i.e. the square roots of negative eigenvalues) are reported as negative frequencies.

⁶ A brief summary is reported here, where only the case of the lowest temperature ($T = 0.46$) is examined. The simulation was performed in the NVE ensemble, so the fluctuations in the ‘I’-potential energy were equivalent to the fluctuations in the kinetic energy. From the ‘I’-potential energy values, the mean potential energy and its standard deviation were estimated. From the mean temperature or the value of the total energy, the mean kinetic energy and its standard deviation (equal to the standard deviation of the potential energy) were derived. The classical vibrational potential energy was assumed to be equal to the kinetic energy and the contributions of diffusive modes were neglected at this temperature. The combined fluctuations of the potential and kinetic energy were estimated by considering the two sources as statistically independent. If no activated process is necessary to reach a saddle point, the saddle point energies must be in the usual fluctuation range. With a fluctuation of two standard deviations, 71.6% of saddle points can be reached, and 95.2% with three standard deviations. It must be noted that the microcanonical ensemble was used to calculate this estimate, whereas the fluctuations in total energy must also be taken into account in real systems. That further favours an essential entropy barrier explanation. Large contributions from activated processes are probably confined to low-temperature glassy phases.

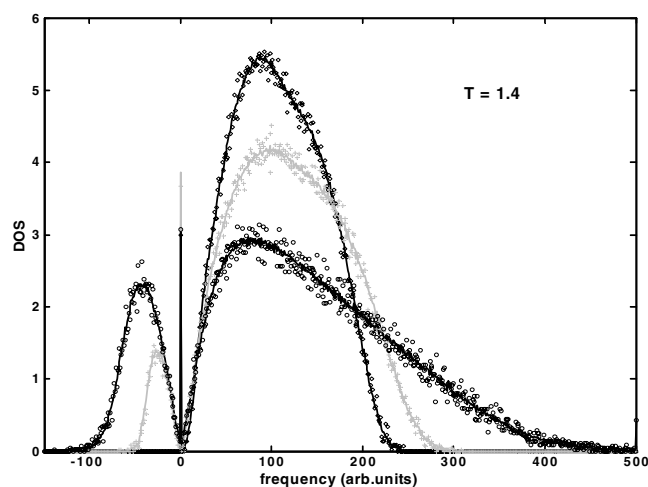


Figure 7. The average DOS at intermediate temperature (liquid regime) from the normal-mode analysis performed on the subset of different configurations giving rise to true saddles: ‘*I*’ (open circles), the true saddle (grey crosses), and the potential minimum (open diamonds) configurations. The average DOS from all the configurations investigated at this temperature are reported as in figure 2, i.e. ‘*I*’ (solid curve), ‘*W*’ (dotted grey line), and ‘*V*’ (dashed curve). Within the statistical uncertainties, the DOS are equal to those obtained from the true-saddle subset.

In figure 6 we report the histogram of the average vibrational density of states (DOS) at two extreme temperatures. From the figure, we can infer that on lowering the temperature, all three DOS will collapse to a single one (when the glass will be confined to a single minimum). In the supercooled regime, approaching T_c , the ‘*W*’-DOS from quasi-saddles becomes more and more similar to the ‘*V*’-DOS from potential minima. At $T = 0.46$, the ‘*W*’-DOS is nearly coincident with the ‘*V*’-DOS while the ‘*I*’-DOS of the initial equilibrium configuration still remains separated. We want to underline that in the channel of the histogram around zero frequency, we found always the three eigenvalues connected to the three translational invariants; for quasi-saddles (not true saddles), another zero-frequency eigenvalue is found due to the change of curvature in one direction of the potential energy hypersurface. This is why the zero channel of the ‘*W*’-DOS has nearly four eigenvalues.

In figure 7, the three DOS calculated from only the true-saddle configurations, i.e. those configurations for which the forces at ‘*W*’-points are really vanishing, are shown and compared with the DOS averaged over all configurations. We want to stress that within the statistical uncertainties the three DOS are not dependent on the chosen subset. This is not obvious for the ‘*W*’-DOS and it is an important result of our study: at least with respect to the distribution of vibrational frequency, true saddles and quasi-saddles share the same information.

Even if the ‘*W*’- and ‘*V*’-DOS seem to be very similar near T_c (see the lower panel of figure 6), there are significant differences at low frequency. In figure 8, we reported the reduced density of states (RDOS) at low frequencies for the three configurations at $T = 0.48$, i.e. the DOS divided by the frequency squared. In the Debye solid approximation the reduced density is a constant, while the well-known ‘boson peak’ is found in real glasses. In the supercooled regime of figure 8, a peak is clearly visible in the ‘*V*’-RDOS, starts to appear in ‘*W*’-RDOS, but is (as yet) completely absent in the ‘*I*’-RDOS.

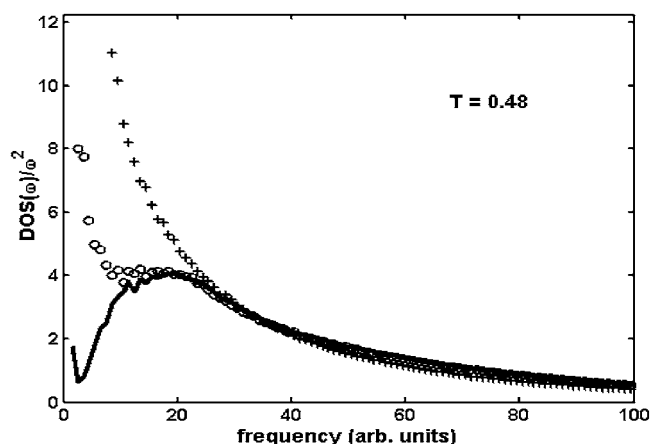


Figure 8. The average reduced DOS in the supercooled regime from the configurations ‘I’ (crosses), ‘W’ (circles), and ‘V’ (solid curve).

4. Conclusions

We have investigated the dynamics of model glass-forming liquids in terms of the PEL by investigating numerous independent configurations at different temperatures in the liquid and supercooled regimes. Potential energy minima, quasi-saddles, and true saddles are derived from equilibrium configurations. The temperature behaviours of the potential energy, saddle order, Cartesian distance, and vibrational DOS for equilibrium, quasi-saddle, and minimum configurations have been studied. On average, the quasi-saddles at low temperatures lie on a more steeply sloping hypersurface compared to those at high temperatures. The number of true saddles is a decreasing function of temperature, so it is important to establish that it is possible also to extract information about the dynamics of the system from the quasi-saddle configurations. It has been demonstrated that the vibrational DOS is practically the same for true and quasi-saddles. At different temperatures, different regions of the PEL are statistically visited by the system, due to the accessible configuration volume growing exponentially with the temperature. The potential energy and the number of unstable directions (i.e. negative eigenvalues) are statistically correlated both for saddles and equilibrium configurations, but at the same potential energy, saddles and equilibrium configurations have different numbers of negative eigenvalues, at least in the liquid–supercooled region investigated. An excess DOS at low frequency is always present in the system investigated, but a ‘boson peak’-like structure is clearly visible only in the DOS derived from potential energy minima.

Acknowledgment

This work was realized with the financial support of MURST.

References

- [1] Goldstein M 1969 *J. Chem. Phys.* **51** 3728
- [2] Keyes T 1997 *J. Chem. Phys.* **101** 2921
- [3] Donati C, Sciortino F and Tartaglia P 2000 *Phys. Rev. Lett.* **85** 1464
- [4] Kurchan J and Laloux L 1996 *J. Phys. A: Math. Gen.* **29** 1929
- [5] Cavagna A, Giardinà I and Parisi G 1998 *Phys. Rev. B* **57** 11251

-
- [6] Angelani L, Di Leonardo R, Ruocco G, Scala A and Sciortino F 2000 *Phys. Rev. Lett.* **85** 5356
 - [7] Broderix K, Bhattacharya K K, Cavagna A, Zippelius A and Giardina I 2000 *Phys. Rev. Lett.* **85** 5360
 - [8] Shah P and Chakravarty C 2001 *J. Chem. Phys.* **115** 8784
 - [9] Cavagna A 2001 *Euro. Phys. Lett.* **53** 490
 - [10] Grigera T S, Cavagna A, Giardina I and Parisi G 2002 *Phys. Rev. Lett.* **88** 55502
 - [11] Kob W and Andersen H C 1995 *Phys. Rev. E* **51** 4626
 - [12] Schroeder T B, Sastry S, Dyre J C and Glotzer S C 2000 *J. Chem. Phys.* **112** 9834
 - [13] Doye J P K and Wales D J 2002 *J. Chem. Phys.* **116** 3777
 - [14] Sampoli M 2003 at press
 - [15] Sastry S, Debenedetti P G, Stillinger F H, Schroeder T B, Dyre J C and Glotzer S C 1999 *Physica A* **270** 301
 - [16] Götze W and Sjögren L 1992 *Rep. Prog. Phys.* **55** 241
 - [17] Sampoli M 2003 at press